Applicability of geometrical optics to in-plane liquid-crystal configurations

M. Sluijter,[1,*] M. Xu,[2] H. P. Urbach,[2] and D. K. G. de Boer[1]

[1]*Philips Research Europe, High Tech Campus 34, MS 31, 5656 AE Eindhoven, The Netherlands*
[2]*Optics Research Group, Delft University of Technology, Department Imaging Science and Technology, Lorentzweg 1, 2628 CJ Delft, The Netherlands*
**Corresponding author: Maarten.Sluijter@philips.com*

Received September 1, 2009; revised December 10, 2009; accepted December 12, 2009; posted January 7, 2010 (Doc. ID 116390); published February 4, 2010

We study the applicability of geometrical optics to inhomogeneous dielectric nongyrotropic optically anisotropic media typically found in in-plane liquid-crystal configurations with refractive indices $n_o=1.5$ and $n_e=1.7$. To this end, we compare the results of advanced ray- and wave-optics simulations of the propagation of an incident plane wave to a special anisotropic configuration. Based on the results, we conclude that for a good agreement between ray and wave optics, a maximum change in optical properties should occur over a distance of at least 20 wavelengths. © 2010 Optical Society of America

OCIS codes: 080.3095, 160.1190, 260.1440.

In geometrical optics, optical laws are obtained in the limit where the wavelength of the light vanishes. Also, the material properties are allowed to change with position, provided that the change is sufficiently small over the distance of a wavelength. One important question that has not received much attention so far is how much change in the material properties per unit wavelength is allowed in geometrical optics. In this Letter, our purpose is to provide some insight into this subject for typical in-plane (dielectric nongyrotropic) liquid-crystal configurations with refractive indices $n_o=1.5$ and $n_e=1.7$ and give a first approximation to the maximum change in material properties per unit wavelength that is allowed in geometrical optics.

If the wave character of light is taken into account, a widely used approach consists of expanding the wave amplitude in terms of $1/(ik_0)$, called a Debye expansion (cf. [1], p. 7). When we substitute this expansion into the Maxwell equations, we obtain a set of first-order partial differential equations that are called the transport equations [2]. In geometrical optics, the optical wave field satisfies the zeroth-order transport equation. The transport equations of higher order are difficult to solve, and they do not provide additional physical insight into the modeling of anisotropic media. In that sense, the use of the transport equations does not form an attractive route to investigate the applicability of geometrical optics. Other criteria for the applicability of geometrical optics, such as Fresnel zones discussed by Kravtsov and Orlov (cf. [1], p. 80), are also difficult to apply in practice.

A different approach to investigate the validity of geometrical optics can be deduced from the following consideration. Consider an anisotropic medium in which the director (i.e., the local optical axis) is rotated gradually by an angle of 90° over a distance L, see Fig. 1. Then L is the distance over which a maximum change in optical properties occurs (for fixed principal refractive indices). We define the dimensionless wavelength by λ/L, where λ is the wavelength of the light. In the limit where $\lambda/L\to 0$, a medium has homogeneous material properties. The limit where $\lambda/L\to\infty$ corresponds to a discontinuity in the material properties. For sufficiently small λ/L, geometrical optics and wave optics agree. The main question is then up to what value of λ/L we are allowed to apply geometrical optics.

To answer this question, we study the effect of a director profile in the xz plane on the propagation of an incident plane wave. For simplicity, we consider an uniaxially anisotropic medium, but the approach described in this Letter can also be applied to biaxially anisotropic media. The director profile is given by

$$\hat{\mathbf{d}}(x,z)=\cos\theta(x,z)\hat{\mathbf{x}}+\sin\theta(x,z)\hat{\mathbf{z}}, \tag{1}$$

with the angle $\theta(x,z)$ defined by

$$\theta(x,z)=\frac{\pi}{4}\left[1-\cos\left(\frac{2\pi x}{T}\right)\right]\sin\left(\frac{\pi z}{D}\right), \tag{2}$$

where D is the thickness and T is the period of the director profile. The corresponding dielectric permittivity tensor is given by

$$\epsilon(x,z)=\begin{pmatrix} n_e^2\cos^2\theta(x,z)+n_o^2\sin^2\theta(x,z) & 0 & \Delta\epsilon\cos\theta(x,z)\sin\theta(x,z) \\ 0 & n_o^2 & 0 \\ \Delta\epsilon\cos\theta(x,z)\sin\theta(x,z) & 0 & n_e^2\sin^2\theta(x,z)+n_o^2\cos^2\theta(x,z) \end{pmatrix}, \tag{3}$$

0146-9592/10/040487-3/$15.00

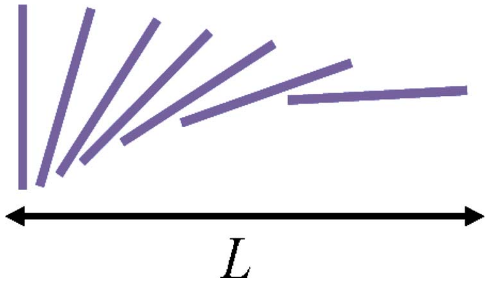

Fig. 1. (Color online) Rotation of the director by 90° over a distance L. Hence L is the distance over which a maximum change in optical properties occurs.

where $\Delta\epsilon = n_e^2 - n_o^2$ and the ordinary and extraordinary indices of refraction are defined $n_o = 1.5$ and $n_e = 1.7$ (TL213 liquid crystal), respectively. One period of the director profile $\hat{\mathbf{d}}(x,z)$ is depicted in Fig. 2 for $T=20$ and $D=20$. We choose this fictitious director profile because it has the general properties we are looking for; the director is gradually rotated by 90° over a distance $D/2$ in the z direction halfway each period (e.g., at $x=30$) and twice each period in the x direction at $z=D/2$. In this case, the gradual rotation of $\hat{\mathbf{d}}$ is defined by goniometric functions but could also be defined by, e.g., linear functions. Finally, we see that the director is in the x direction for $z=0$, $z=D$, and $x=kT$, with $k \in \mathbb{N}$. The surrounding medium ($z<0$ and $z>D$) is isotropic with $n=1.0$. This optical system is somewhat similar to that of an in-plane-switching liquid-crystal cell [3].

We will use the advanced ray-tracing procedure discussed in [4] to simulate how an incident plane wave propagating in the z direction and polarized in the x direction is affected by the periodic director profile. Figure 2 shows the curved-ray paths of extraordinary light rays inside one period of the director profile.

An explanation for the diverging behavior can be found in the fact that light bends toward regions of high refractive index. We can explain this by examining an effective index of refraction n_{eff} at each position (x,z) of extraordinary light rays with propagation direction $\hat{\mathbf{s}}_e(x,z) = \hat{\mathbf{z}}$. Then we have $n_{\text{eff}}(x,z) = \sqrt{n_o^2 n_e^2 / \cos^2(\theta) n_o^2 + \sin^2(\theta) n_e^2}$ with θ given by Eq. (2). The maximum of n_{eff} lies in the periphery of one period, since there $n_{\text{eff}} = n_e$. In the center we have $n_{\text{eff}} = n_o$. As a result, a light ray entering the director profile at, for example, $x=32$ penetrates the region of low refractive index in the center and then bends toward the nearby region of high refractive index at the right. Hence the ray paths show a diverging effect.

At $z=D$ the extraordinary intensity transmittance factor T_e of the rays is calculated (taking into account single reflections),

$$T_e = \frac{S_z^t}{S_z^{\text{inc}}}, \tag{4}$$

where S_z^t is the z component of the transmitted Poynting vector at $z=D$ and S_z^{inc} the z component of the incident Poynting vector at $z=0$. At $z=D$ the rays (a total number of 1.44×10^6, each having a weight factor T_e) are collected in intervals of length $\Delta x = 0.05$. Then the total number of rays collected by an interval is a measure for the intensity (W/m^2). Hence we obtain a (scaled) spatial intensity distribution I that is periodic with period T. The result is depicted in Fig. 3. Clearly we observe peak intensities near the edges of the period T and a low intensity in the middle.

In what follows, we present results of wave-optics simulations according to an advanced rigorous inhouse numerical simulation program based on the FEM developed jointly by Philips Research and Delft University of Technology [5]. This method enables in particular the numerical simulation of the electromagnetic field inside an inhomogeneous anisotropic medium.

In the FEM simulations the wavelength of the incident plane wave in the surrounding medium (where $n=1$) is 500 nm. The electromagnetic field of the propagating plane wave is calculated at $z=D$ after re-

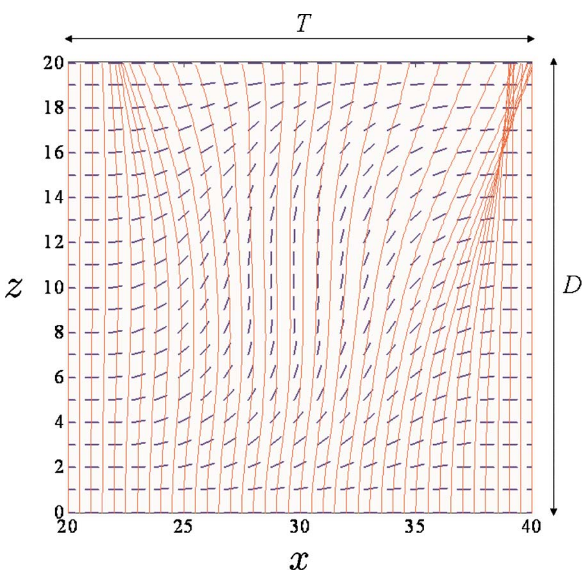

Fig. 2. (Color online) Periodic director profile (indicated by the bars) for $x \in [T, 2T]$ with the ray paths of extraordinary light rays indicated by the curved lines. The light rays are at normal incidence with the plane $z=0$.

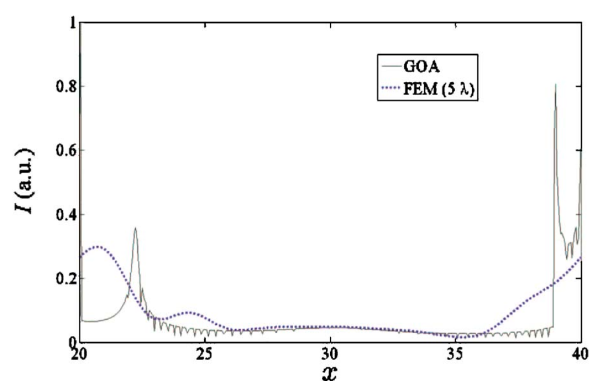

Fig. 3. (Color online) Spatial intensity distributions according to the finite-element-method (FEM) simulations and the ray-tracing simulations (GOA) for $T=5\lambda$. This corresponds to a computational domain of 2.5×2.5 μm, assuming $\lambda = 500$ nm.

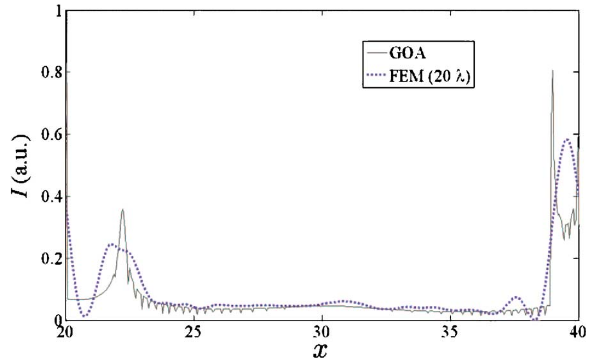

Fig. 4. (Color online) Spatial intensity distributions for $T=20\lambda$. Then a period of the director profile corresponds to a computational domain of 10×10 μm.

fraction at the interface. There the ratio between the z component of the transmitted and incident Poynting vector is calculated as a function of position x, and the resulting spatial intensity distribution reads

$$I^{\mathrm{FEM}}(x)=\frac{S_z^t}{S_z^{\mathrm{inc}}}. \qquad (5)$$

The FEM simulations are performed for different values of the period T. First, we take $T=D=5\lambda$ and with $\lambda=500$ nm, this corresponds to a computational domain of 2.5×2.5 μm. The spatial intensity distributions of the ray-optics and wave-optics simulations are depicted in Fig. 3. Similar results for $T=20\lambda$, $T=40\lambda$, and $T=60\lambda$ are depicted in Figs. 4–6, respectively.

From the results we conclude that qualitatively, there is a match between the FEM simulations and the ray-tracing simulations. Quantitatively, there is a good match for $T=40\lambda$ and $T=60\lambda$. However, the match is not perfect. This is because the FEM simulations include diffraction effects. Diffraction effects are likely to occur, especially in the region where ray paths intersect one another. This can be seen in the right upper corner in Fig. 2, where the FEM simulations show an intensity distribution that resembles a diffraction pattern. This explains the incongruence between the FEM simulations and ray-optics simulations in this particular region. We can also see that the agreement between the FEM simulations and the

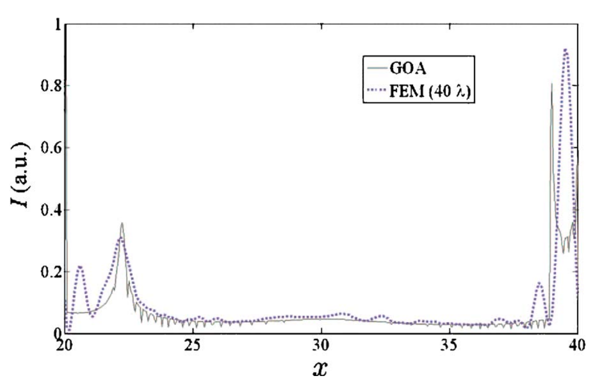

Fig. 5. (Color online) Spatial intensity distributions for $T=40\lambda$. Now the computational domain of the FEM is 20×20 μm.

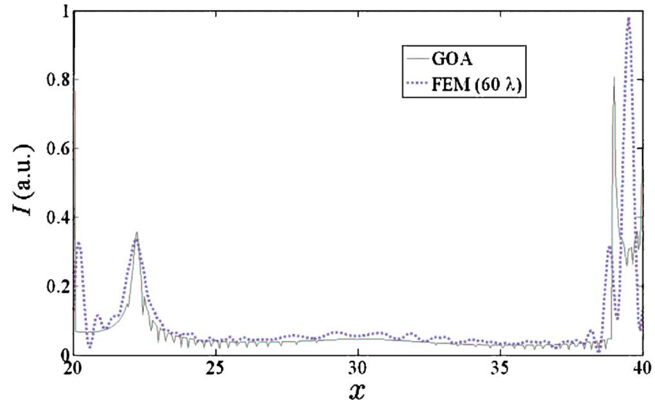

Fig. 6. (Color online) Spatial intensity distributions for $T=60\lambda$. The computational domain of the FEM has reached a maximum of 30×30 μm owing to memory constraints.

Table 1. Values for T, L and Ratio λ/L Used in the Simulations

T (λ)	L (λ)	L (μm)	$\frac{\lambda}{L}$
5	2.5	1.25	0.400
20	10	5.0	0.100
40	20	10.0	0.050
60	30	15.0	0.033

ray-tracing simulations improves when T increases. This observation is in line with what one would expect, since the ratio λ/L decreases with increasing T. The values for the period T and the corresponding ratio λ/L are listed in Table 1.

Based on the results, we formulate the following criterion. If $L>20\lambda$ or $\lambda/L<0.05$, ray optics and wave optics are in good agreement, both qualitatively and quantitatively. If $L<20\lambda$, the correlation between ray and wave optics decreases. However, a qualitative agreement between ray and wave optics might still be established for values of L below 20 wavelengths. This criterion applies if L corresponds to a director rotation of 90°. If L corresponds to a rotation of less than 90°, larger values for λ/L are allowed.

We conclude that we have found a criterion ($\lambda/L<0.05$) for the applicability of geometrical optics for typical inhomogeneous in-plane liquid-crystal configurations with refractive indices $n_o=1.5$ and $n_e=1.7$.

References

1. Y. A. Kravtsov and Y. I. Orlov, *Geometrical Optics of Inhomogeneous Media* (Springer-Verlag, 1990).
2. M. Kline and I. W. Kay, *Electromagnetic Theory and Geometrical Optics* (John Wiley & Sons, 1965).
3. T. C. Kraan, T. van Bommel, and R. A. M. Hikmet, J. Opt. Soc. Am. A **24**, 3467 (2007).
4. M. Sluijter, D. K. G. de Boer, and J. J. M. Braat, J. Opt. Soc. Am. A **25**, 1260 (2008).
5. M. Xu, L. Sio, R. Caputo, C. P. Umeton, A. J. H. Wachters, D. K. G. de Boer, and H. P. Urbach, Opt. Express **16**, 14532 (2008).